Effect of a nonspiking neuron on motor patterns of the leech

Mariano J. Rodriguez, Rodrigo J. Alvarez and Lidia Szczupak

J Neurophysiol 107:1917-1924, 2012. First published 11 January 2012; doi:10.1152/jn.01070.2011

Journal of Neurophysiology publishes original articles on the function of the nervous system. It is published 12 times a year (monthly) by the American Physiological Society, 9650 Rockville Pike, Bethesda MD 20814-3991. ISSN: 0022-3077, ESSN: 1522-1598. Visit our website at http://www.the-aps.org/.

J Neurophysiol 107: 1917–1924, 2012.
First published January 11, 2012; doi:10.1152/jn.01070.2011.

Effect of a nonspiking neuron on motor patterns of the leech

Mariano J. Rodriguez,* Rodrigo J. Alvarez,* and Lidia Szczupak
Departamento de Fisiología, Biología Molecular y Celular, FCEN-UBA, IFIBYNE UBA-CONICET, Buenos Aires, Argentina

Submitted 23 November 2011; accepted in final form 6 January 2012

Rodriguez MJ, Alvarez RJ, Szczupak L. Effect of a nonspiking neuron on motor patterns of the leech. *J Neurophysiol* 107: 1917–1924, 2012. First published January 11, 2012; doi:10.1152/jn.01070.2011.— Premotor and motoneurons could play regulatory roles in motor control. We have investigated the role of a premotor nonspiking (NS) neuron of the leech nervous system in two locomotive patterns: swimming and crawling. The NS neuron is coupled through rectifying electrical junctions to all the excitatory motoneurons examined. In addition, activation of motoneurons evokes chemically mediated inhibitory responses in NS. During swimming and crawling, the NS membrane potential (Vm_{NS}) oscillated phase locked to the motor output. Hyperpolarization or depolarization of NS had no effect on swimming, but hyperpolarization of NS slowed down the crawling activity and decreased the motoneuron firing frequency. Depolarization of NS increased the motoneuron activity, and, at stages where the crawling pattern was fading, depolarization of NS reinstated it. Future work should determine if NS is actually a member of the central pattern generator or a regulatory element.

premotor; motoneurons

OUR KNOWLEDGE ON THE STRUCTURE of motor systems has progressed remarkably in the past decades (Grillner 2003; Katz 1996; Orlovsky et al. 1999; Tresch et al. 2002), and new concepts that were absent in early models were introduced. Among these new concepts, we have learned that lower levels of this hierarchical organized system, premotor neurons and motoneurons, form modular circuits that can be considered as building blocks of motor behaviors (Fetz et al. 2000; Poppele 2003; Tresch et al. 2002). This indicates that premotor and motoneurons could play regulatory roles in motor control.

Invertebrate nervous systems have pioneered the research in motor control due, mainly, to the relative simplicity of the organisms themselves, that make feasible the recording of higher and lower control levels simultaneously in an experimental preparation. The leech has been an outstanding example in this respect (Briggman and Kristan 2006; Cymbalyuk et al. 2002; Gaudry and Kristan 2009).

Wadepuhl (1989) discovered in the leech a nonspiking neuron with widespread connectivity with motoneurons. This neuron, the nonspiking (NS) cell, is coupled through rectifying electrical junctions to all the excitatory motoneurons examined (Rela and Szczupak 2003; Rodriguez et al. 2009; Wadepuhl 1989). These junctions conduct when the membrane potential of the NS cell is more negative than that of motoneurons (Rela and Szczupak 2007; Rodriguez et al. 2009). In addition, activation of motoneurons evoke chemically mediated inhibitory responses in NS (Rela and Szczupak 2003; Rodriguez et al. 2009).

The extensive synaptic connectivity between NS and motoneurons led us to hypothesize that this neuron plays a role in the execution of motor behaviors. Here we analyze its role in two prominent motor patterns: swimming and crawling. Both are rhythmic behaviors that activate overlapping populations of motoneurons, with different spatio-temporal patterns. Swimming is a relatively fast locomotor behavior (Kristan et al. 1974), while crawling is a much slower displacement that allows exploratory intervals (Stern-Tomlinson et al. 1986). The results indicate that while NS plays no role in swimming, it modulates the central pattern generator (CPG) that controls crawling. This is the first report on a neuron that can regulate the crawling motor pattern.

MATERIALS AND METHODS

Biological preparation. Leeches (*Hirudo sp.*) weighing 2–5 g were obtained from a commercial supplier (Leeches USA, Westbury, NY) and maintained at 15°C in artificial pond water. The leech nervous system is composed of 21 midbody ganglia, aligned between a head and a tail brain. Each midbody ganglion innervates one body segment and contains all the corresponding sensory and motor neurons (Muller et al. 1981). All motoneurons project their axons through specific, mostly contralateral, peripheral nerves.

Swimming was studied in an isolated chain of ganglia spanning from midbody ganglion 2 to the tail brain; crawling was studied in single isolated midbody ganglia. The tissue was bathed in normal saline (in mM: 115 NaCl, 4 KCl, 1.8 $CaCl_2$, 1 $MgSO_4$, 10 Tris base, 10 glucose; pH 7.4) at room temperature (20–25°C). In all cases, the sheath covering the recorded ganglia was removed.

Electrophysiology. Intracellular somatic recordings of NS neurons were made with microelectrodes pulled from borosilicate capillary tubing (FHC, Brunswick, ME) filled with a 3 M potassium acetate solution (resistance 20–40 MΩ). The electrodes were connected to an Axoclamp 2B amplifier (Axon Instruments, Union City, CA) operating in bridge mode. Extracellular activity was recorded in peripheral nerves, using suction electrodes connected to a differential AC amplifier (Neuroprobe 1700; AM-Systems, Carlsborg, WA). Intra- and extracellular recordings were digitized using a Digidata 1320 interface (Axon Instruments) and acquired using Clampex protocols (pClamp 9.2, Axon Instruments) at sampling rates of 5–10 kHz.

All neurons recorded intracellularly were recognized by their soma location and their electrophysiological properties. The spikes of dorsal longitudinal excitor motoneuron 3 (DE-3) can be recorded in the contralateral dorsal posterior (DP) nerve (Ort et al. 1974). To evoke crawling, the ganglion was continuously superfused at a rate of 1–2 ml/min with saline solution containing 75 μM dopamine (Puhl and Mesce 2008); to evoke swimming, a 0.5- to 1-s pulse train (1–5 V, 1 ms, 10–20 Hz) was applied to a DP nerve of ganglia 16 to 18 through a suction electrode, via a stimulus isolator (model A360; WPI, Sarasota, FL), and triggered by the acquisition software. In the study of crawling, each ganglion was superfused with dopamine (DA)-containing saline for ~30 min. A single crawling episode was evoked in each ganglion.

Data analysis. Data analysis was performed using Clampfit 9 (Axon Instruments). Spikes were detected using amplitude threshold,

* M. J. Rodriguez and R. Alvarez contributed equally to this work.

Address for reprint requests and other correspondence: L. Szczupak, Ciudad Universitaria, Pabellón II, piso 2, CABA 1428, Buenos Aires, Argentina (e-mail: szczupak@retina.ar).

or, when necessary, amplitude window (setting upper and lower limits). The instantaneous firing frequency was calculated as the inverse of the period between a spike and the one preceding it. A burst is defined as a series of at least five successive spikes that exhibited an instantaneous firing frequency larger than 1 Hz. The mean firing frequency of a burst was calculated as the mean of the instantaneous firing frequency of the spikes that constituted the burst. The cycle period was measured as the time between the middle spike in successive DP bursts of swimming (Kristan et al. 1974) and as the time between the first spike of successive bursts of crawling motoneurons. Some traces were smoothed with a running average: the number of data points was reduced by the factor indicated in the figure legend and replaced by the average of the group of points. Unless otherwise stated, data are presented as means ± SE.

Statistical tests and their outcome (P value, n = sample size) are indicated in RESULTS and in the figure legends.

RESULTS

Activity of NS during swimming. Leeches swim by undulating their body in the dorso-ventral plane. This is achieved by the antiphasic rhythmic activity of the motoneurons that contract the dorsal and the ventral longitudinal muscles (Stent et al. 1978). The swimming motor pattern can be studied in the isolated nerve cord, stimulating a rear nerve and recording the activity of the motoneurons in the midbody roots (see MATERIALS AND METHODS).

We analyzed the electrophysiological activity of NS neurons in the course of swimming episodes. Figure 1*A* presents an extracellular recording of a DP nerve in the middle of the cord, showing bursts of the DE-3 motoneuron in response to electrical stimulation of a posterior DP nerve. In phase with DE-3, the simultaneous extracellular recording of a posterior branch of the posterior nerve (PP) shows the activity of DE-5 and DE-7, and out of phase with DE-3 the activity of the ventral excitors, cell 4 and 8 (Ort et al. 1974). Concurrent intracellular recording of an NS cell shows that the stimulation evoked a sharp depolarization that decayed to a level above the resting baseline. The membrane potential of NS (Vm_{NS}) remained at this value for the duration of the swimming episode (Fig. 1*A*). On top of the sustained depolarization, Vm_{NS} oscillated at a constant phase relation to the swimming rhythm (Fig. 1*B*). Figure 1*C* shows a box-Whisker plot describing the distribution of Vm_{NS} for 5 s prior to the stimulus and for 5 s once the

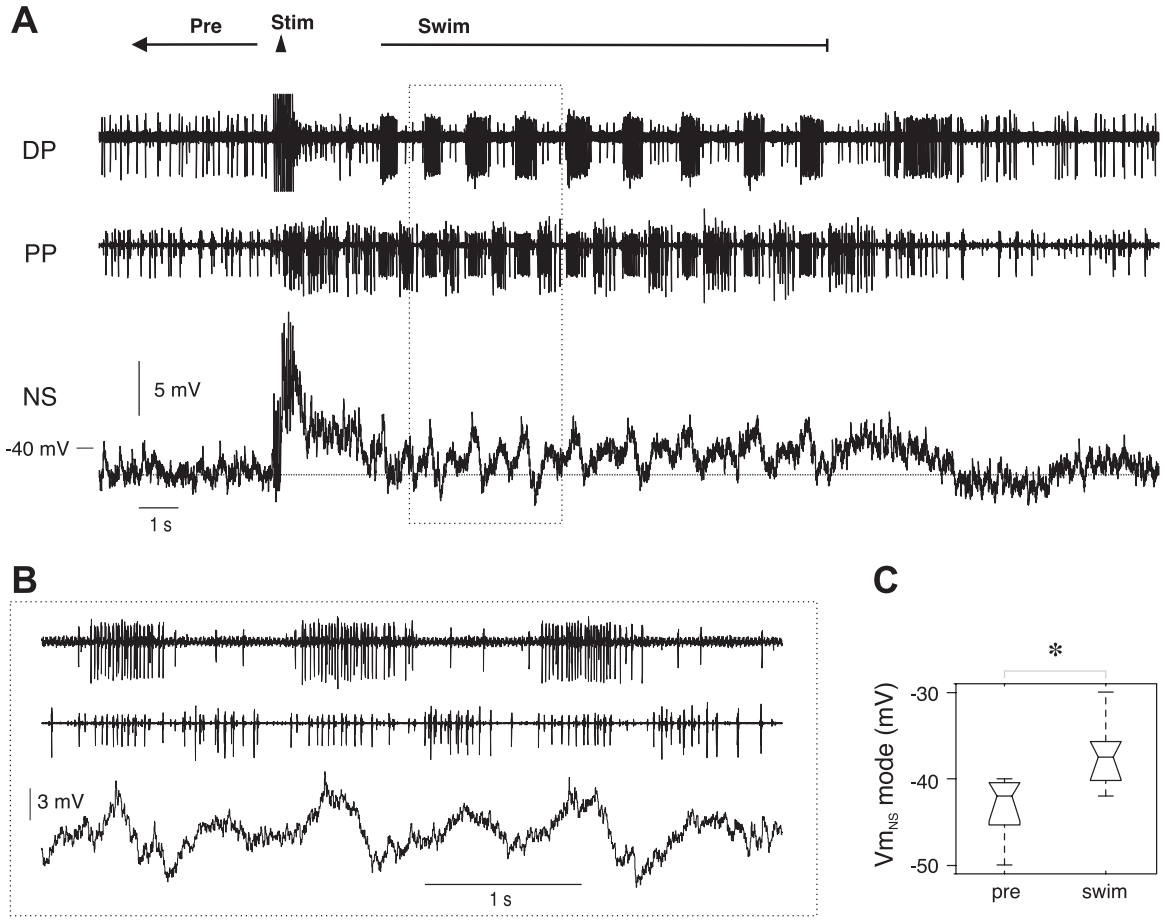

Fig. 1. Nonspiking (NS) neuron activity during swimming. *A*: simultaneous extracellular recordings of a dorsal posterior (DP) nerve and a posterior (PP) nerve and intracellular recording of an NS cell in midbody ganglion 10, in an isolated chain of ganglia (see MATERIALS AND METHODS). Stimulation (3 V, 1-ms pulses at 20 Hz) applied to a DP nerve of midbody ganglion 18 evoked the swimming motor pattern. The timing of the stimulation (Stim) is indicated by the triangle above the recordings. The big spikes of dorsal longitudinal excitor motoneuron 3 (DE-3) dominate the DP activity. The big spikes in the PP nerve in phase with the DE-3 spikes correspond to dorsal excitors cells 5 and 7; the big spikes in anti-phase with DE-3 correspond to the ventral excitors cells 4 and 8. A reference Vm value is indicated on the *left* of the NS recording. *B*: expanded view of the segment enclosed in the line box in *A*. *C*: box-whisker plot describing the distribution of Vm_{NS} values during 5 s prior to the stimulus (pre) and the first 5 s of the swimming motor pattern (swim). In each case, we measured the mode of the Vm_{NS} values during those periods. $N = 7$ preparations; $^*P = 0.016$, Wilcoxon signed-rank test.

swimming rhythm was established. The median value of Vm_{NS} mode shifted by ~5 mV.

The effect of NS on swimming. Because Vm_{NS} modulates the effective electrical coupling among motoneurons, it was of interest to analyze the influence of this variable on the swimming motor pattern. If Vm_{NS} is set above the resting potential, the electrical coupling among motoneurons is counteracted by a network of chemical connections, whereas shifting Vm_{NS} to −80 mV unmasks the electrical coupling (Rela and Szczupak 2003; Rodriguez et al. 2009). To study the effect of shifting Vm_{NS} on the swimming motor output, we evoked swimming after setting Vm_{NS} at ~−80 and −20 mV. Figure 2*A* presents two representative examples of these experiments. The most obvious effect of this manipulation was seen in the response of NS itself. The amplitude of the transient depolarization caused by the stimulus and of the sustained depolarization during swimming were larger as Vm_{NS} was set at the more negative potential. On the other hand, the rhythmic oscillations in Vm_{NS} were more pronounced when the cell was set at the more positive potential. These are expected effects for chemically mediated responses with positive and negative reversal potentials, respectively.

However, this Vm_{NS} manipulation had no effect on the motor output. We analyzed the length of the episodes, the burst duration, and the period and the firing frequency of DE-3. Vm_{NS} did not affect any of these parameters (Fig. 2*C*).

Activity of NS during crawling. A crawling motor pattern was elicited in isolated midbody ganglia by the application of DA to the bath (Puhl and Mesce 2008). Figure 3 shows a representative extracellular recording of a DP nerve and an intracellular recording of an NS in the course of DA superfusion (see MATERIALS AND METHODS). After a latency, the crawling motor pattern can be recognized as the rhythmic bursting of DE-3 evident in the DP recording (Perez-Etchegoyen et al. 2011). Notice that the period and burst duration during crawling were much longer than during swimming (Fig. 1). In the course of the crawling motor pattern, Vm_{NS} underwent sharp depolarizing and hyperpolarizing oscillations. An expanded view presented in Fig. 3*B* indicates that the NS response was composed of different phases: a barrage of presumably hyperpolarizing postsynaptic potentials in phase with DE-3 bursts, followed by a sustained hyperpolarization (with respect to the pre-DA baseline) that lasted for approximately half the DE-3 silent period, and finally a sustained depolarization that ended at the onset of the DE-3 burst. This general pattern was observed in all the preparations where NS was recorded (n = 19), but the magnitude of each component varied among different preparations.

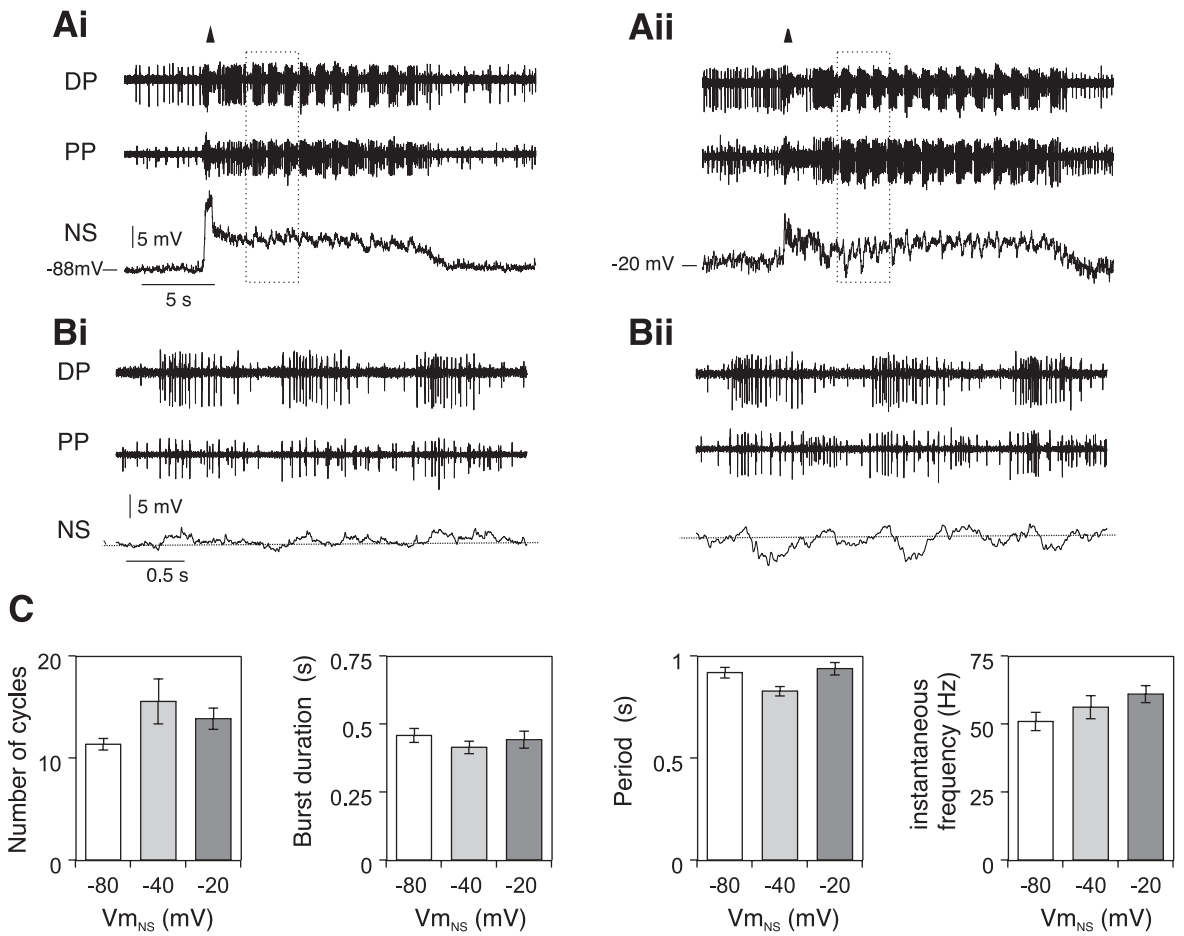

Fig. 2. Effect of Vm_{NS} on swimming. *A*: simultaneous extracellular recordings of a DP nerve and a PP nerve and intracellular recording of an NS cell as the latter was set at ~−80 mV (i) and −20 mV (ii). Same preparation as in Fig. 1. *B*: expanded view of the segments enclosed in the line box in *A*. *C*: the bars present average number of cycles per episode, burst duration, period, and mean instantaneous firing frequency of DE-3 for recordings in which Vm_{NS} baseline before the stimulus was set at ~−80, −40, and −20 mV (n = 7). No statistical differences were found ($P > 0.05$, Wilcoxon test for paired data comparing the 3 possible pairs).

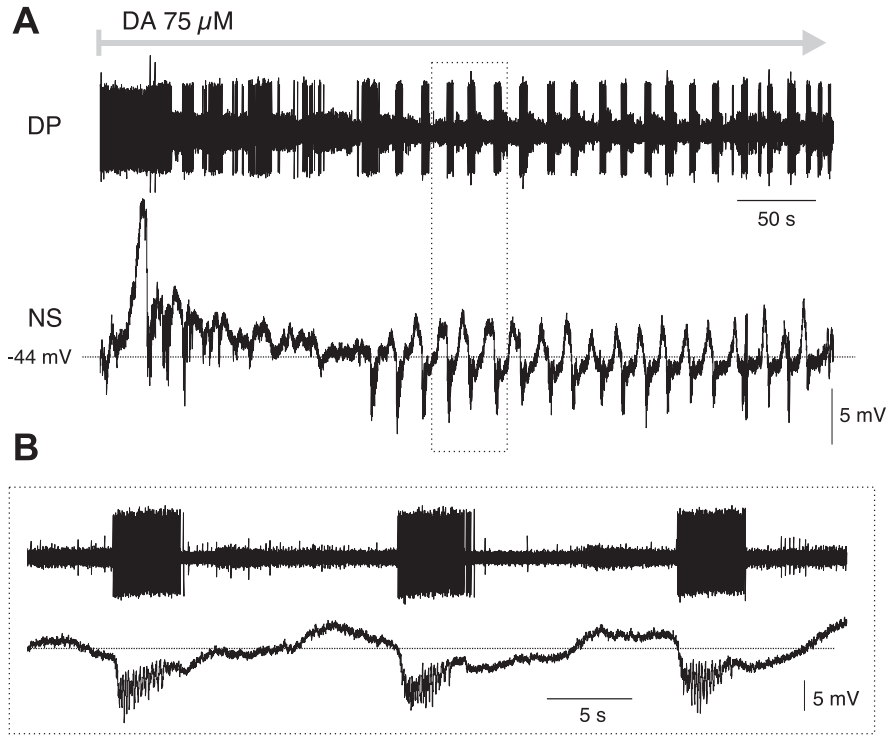

Fig. 3. NS activity during crawling. *A*: simultaneous extracellular recording of a DP nerve and intracellular recording of an NS neuron in an isolated midbody ganglion. The beginning of the trace marks the onset of the superfusion with saline solution containing 75 μM dopamine (DA). *B*: expanded view of the segment enclosed in the line box in *A*.

In the contraction phase of crawling, the activation of dorsal and ventral longitudinal muscle fibers is accompanied by the contraction of the muscle fibers that cause erection of the annuli of the skin and which are controlled by the bilateral pair of annulus erector (AE) motoneurons (Eisenhart et al. 2000). Figure 4*A* presents a simultaneous extracellular recording of a DP nerve and intracellular recordings of AE and NS during a DA-induced crawling episode. The AE firing activity occurred concomitant with DE-3 firing, and the changes of Vm_{AE} were close to a mirror image of Vm_{NS}. Figure 4*B* presents a smoothed version of these recordings, where the negative correlation of the electrical activity of these two neurons becomes more evident. Figure 4*C* shows the cross correlation of these recordings for a segment of the episode of ~4 min. The mean amplitude of the cross correlograms obtained in three simultaneous AE and NS recordings was of ~ -0.7 (-0.67 ± 0.07) and showed a delay of ~0 s (0.2 ± 0.2 s).

The elongation phase of crawling is carried out by the contraction of circular muscles (Eisenhart et al. 2000). Figure 4*D* shows that the excitor of the ventral circular muscles (CV) bursted out of phase with respect to DE-3. In addition, the figure shows simultaneous intracellular recordings of CV and NS, showing a marked correlation between these two neurons (Fig. 4, *D* and *E*) that shows a cross correlation amplitude close to 1 (Fig. 4*F*). The mean amplitude of the cross correlograms obtained in four simultaneous recordings of CV and NS was of ~0.9 (0.85 ± 0.03) with a delay of 0 s (0 ± 0 s).

The effect of NS on crawling. DA-induced crawling episodes lasted ~20 min. This rhythmic activity was not as regular as swimming, and it varied between episodes and within episodes. Thus the strategy used to study the influence of NS on swimming was inadequate to study its influence on crawling. Instead, we chose to inject electrical current pulses in NS during an ongoing episode. Figure 5 presents the extracellular recording of a DP nerve in the course of a crawling episode, during which pulses of -5, -1, and -0.5 nA were injected in NS through an intracellular electrode. The pulses were applied manually for a duration that spanned 3–4 cycles. The graph underneath the recording shows the instantaneous firing frequency of DE-3 as a function of time. Pulses of -5 nA completely shut down the rhythmic activity in DP, turning it silent for the period of current injection ($n = 3$ episodes). In the example of Fig. 5, the -1 nA pulse strongly inhibited the rhythmic pattern. Under this condition, DE-3 fired short bursts of low firing frequency and at longer periods. Similarly, the -0.5 nA pulse allowed the manifestation of short DE-3 bursts that exhibited a low firing frequency, but in this case the bursts occurred at shorter periods.

On the basis of the electrical coupling between NS and DE-3 (Rodriguez et al. 2009), the effect of -5 nA pulses could be interpreted as a direct inhibitory effect of NS on the motoneuron. However, the effect of the -1 nA pulse suggests that this explanation is not sufficient and hinted at an effect of NS on higher control levels (e.g., the CPG). We thus adopted the -1 nA pulses to perform a more systematic analysis of the role of NS on crawling.

The characteristics of crawling changed during an episode. Figure 6*A* shows the evolution of the cycle period, burst duration, and mean firing frequency of DE-3 as a function of cycle number. Because experimental conditions could completely shut down the rhythmic activity, we expressed the cycle period as cycle frequency (1/period). The graphs show that the rhythmic activity sped up with time, while the burst duration became shorter, but the firing frequency of DE-3 remained relatively constant.

To test the effect of -1 nA pulses in the context of this variable rhythmic activity, we repeated the injections two or three times during an episode and analyzed the effect of each pulse, comparing the DP activity before, during, and after the pulse. Figure 6*B* presents the analysis of a representative

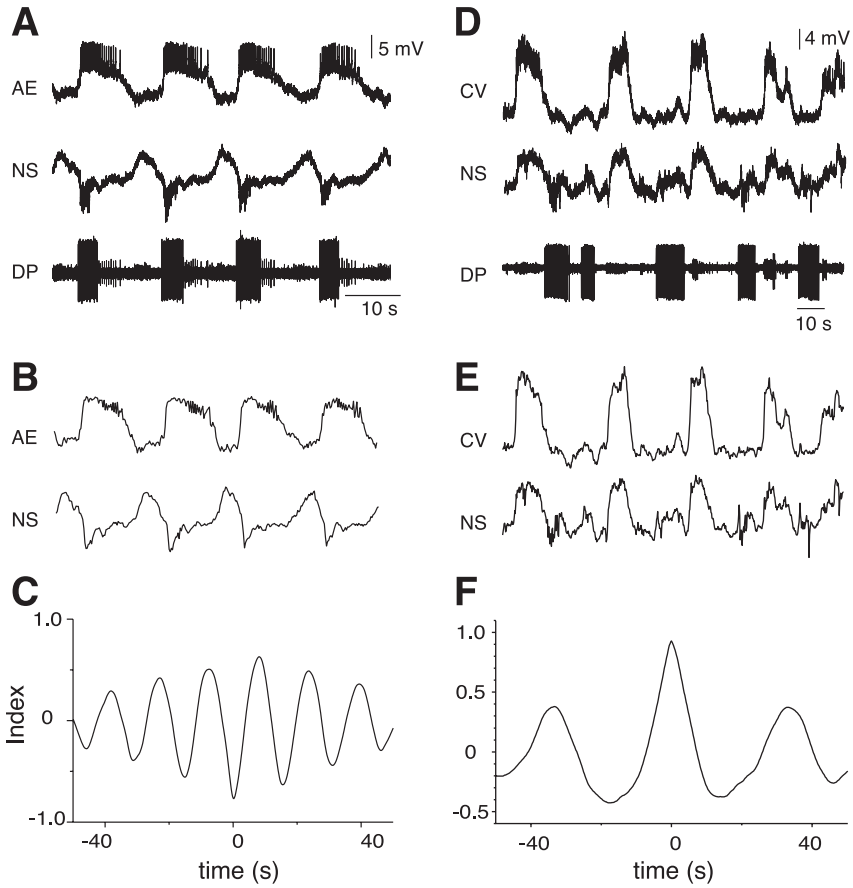

Fig. 4. Correlation of the activity of NS with annulus erector (AE) and ventral circular (CV) motoneurons. *A*: simultaneous intracellular recordings of an AE motoneuron and an NS neuron, and a DP extracellular recording in the course of a DA-induced crawling. *B*: the same intracellular recordings as in *A*, smoothed by a factor of 500 along time. *C*: cross correlation of the smoothed traces shown in *B* (bin width of 200 ms). *D–F*: as in *A–C*, for a CV motoneuron.

example showing the instantaneous firing frequency of DE-3 as a function of time during a DA-induced crawling. The data indicates that in all cases the −1 nA pulse decreased the firing frequency of DE-3, and it also increased the period of the rhythmic activity. Figure 6*C* summarizes the data pooling together the pulses applied to 11 crawling episodes.

The injection of −1 nA pulses in NS caused a significant reduction in the cycle frequency. This effect reversed after the release of the pulse, and, moreover, the cycle frequency after the pulses was significantly higher than before the pulse.

The burst duration was shortened by NS hyperpolarization, but this effect did not reverse after the release of the pulse. Since in the course of DA-induced crawling the burst duration tended to decrease with time (Fig. 6*A*), the effect seen during NS hyperpolarization was probably not caused by Vm_{NS} manipulation. Finally, NS hyperpolarization reversibly diminished the mean instantaneous firing frequency of the DE-3 bursts.

Using a similar protocol, we investigated the effect of depolarizing the NS neuron with 1 nA pulses. Figure 6*D* presents a representative experiment showing that depolarization of NS produced an increase in the firing frequency of DE-3. Figure 6*E* indicates that the cycle frequency increased during NS depolarization, but continued to increase after the end of the pulse, suggesting that NS depolarization had no specific effect on this parameter. Similarly, the burst duration decreased during the pulse, but this effect also followed the natural tendency in the course of crawling (Fig. 6*A*). On the other hand, the firing frequency reversibly increased upon NS depolarization indicating that this was a genuine effect of

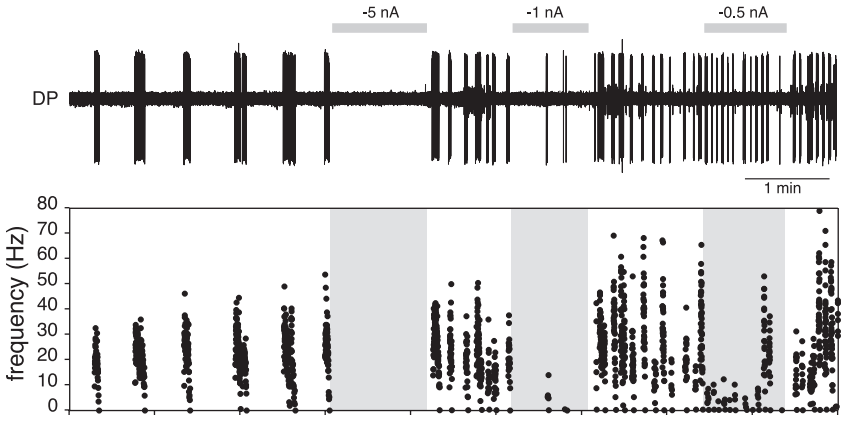

Fig. 5. Effect of NS on crawling. Extracellular DP recording during a DA-induced crawling episode. The horizontal gray bars indicate the timing of current injections into a simultaneously recorded NS neuron. The current intensity is indicated on *top* of the bars. The graph presents the instantaneous firing frequency of DE-3 as a function of time, for the recording segment shown above. The gray shades indicate the time of current injection.

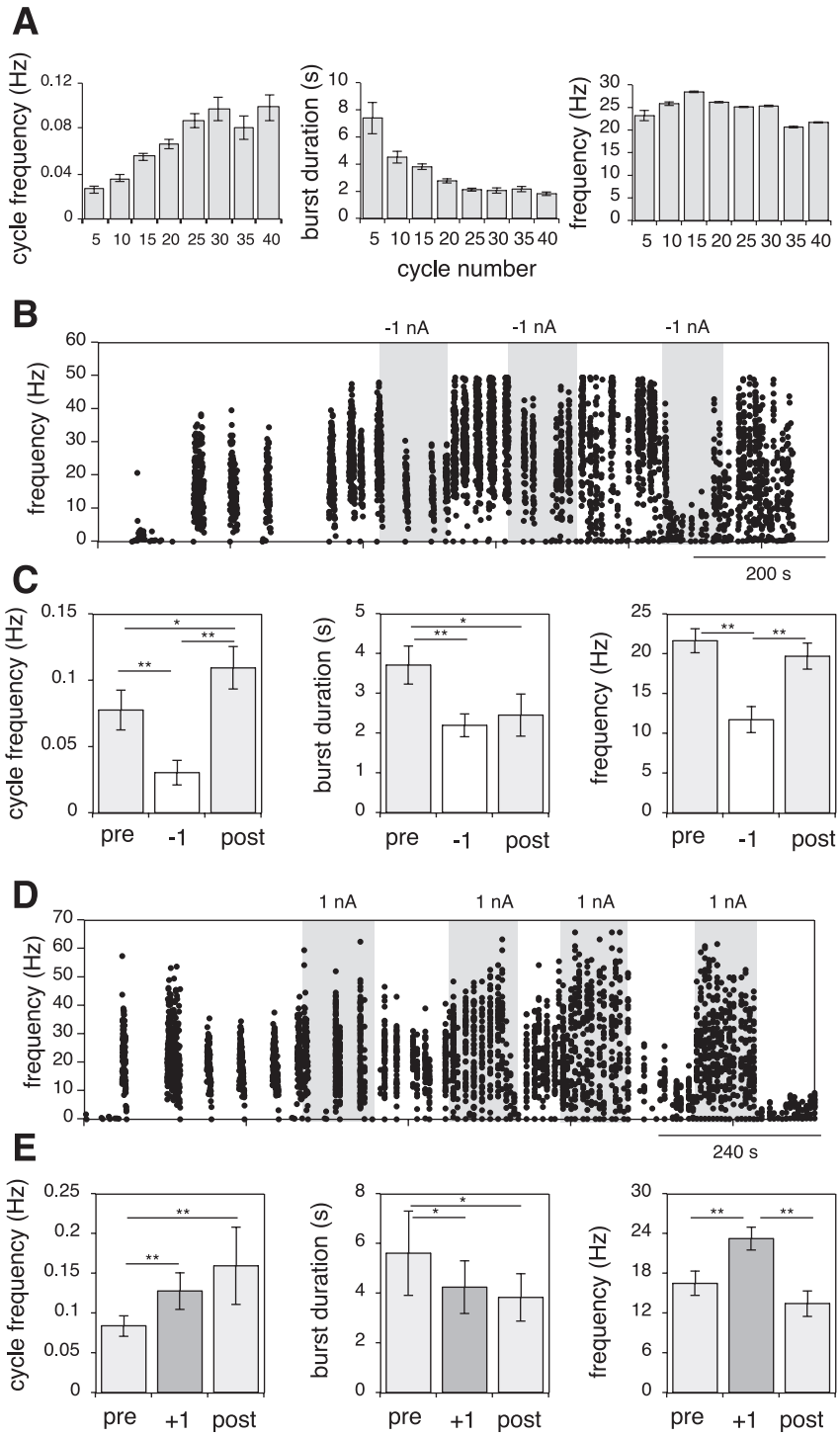

Fig. 6. Analysis of the effect of NS on crawling. *A*: the graphs present the mean cycle frequency (1/period), burst duration, and mean instantaneous spike frequency as a function of the cycle number (5 cycle bins; $n = 10$). *B*: mean instantaneous firing frequency of DE-3 as a function of time during a crawling episode. The gray shades indicate the times of current injections (−1 nA) in NS. *C*: the bars present the cycle frequency, burst duration, and spike frequency measured for 100 s before (pre), during the −1 nA pulse, and for 100 s after (post) the end of the pulse ($n = 11$ episodes). *D* and *E*: as in *B* and *C* for +1 nA ($n = 8$ episodes). $^{**}P < 0.003$ and $^{*}P < 0.014$, Wilcoxon test for paired data. In all cases, a Friedman test was applied to test significant differences between the 3 data sets for each variable.

Vm_{NS} manipulation. When 2 nA pulses were applied, the effect was similar to the one described for 1 nA pulses (data not shown).

The effect of DA usually lasted for ~20 min; after this window of time, DE-3 activity lost the clear bursting pattern and continued to fire at a lower frequency, lacking well-defined silent periods. We considered that the crawling pattern ended when the intervals during which DE-3 remained silent were shorter than 2 s. If NS was depolarized during this phase, the crawling pattern recovered. Figure 7 shows a representative example. At the beginning of this trace, DE-3 fired at a relatively low frequency, and the crawling pattern was already broken down; injecting a 2 nA pulse in NS restored the pattern. Similar observations were made in another eight preparations.

DISCUSSION

The interpretation of the data described in this work has been summarized in the two schemes presented in Fig. 8. Their details will be analyzed throughout the DISCUSSION.

NS activity during motor patterns. In the course of both motor patterns, Vm_{NS} oscillated with each of the rhythmic

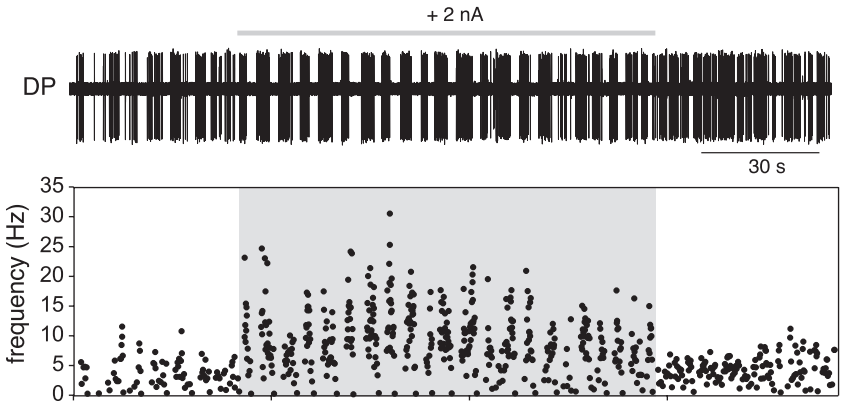

Fig. 7. NS induces the recovery of crawling. The beginning of the trace shows the activity in DP nerve 22 min after the onset of DA superfusion. The gray bar on *top* indicates the timing of a +2 nA pulse in a simultaneously recorded NS neuron. The graph presents the instantaneous firing frequency of DE-3 as a function of time. The gray shade indicates the time of current injection.

patterns. Based on the known motoneuron effect on NS (Rela and Szczupak 2003; Rodriguez et al. 2009; Wadepuhl 1989), we interpret that these oscillations reflect the polysynaptic inhibitory inputs from the motoneurons (Fig. 8, *A* and *B*). During crawling, the concomitant activation of dorsal and ventral excitors could be responsible for the phasic hyperpolarization recorded in NS during the contraction phase (DE-3 burst). This phasic hyperpolarization takes place in the middle of a steadier hyperpolarization. The negative cross correlation between AE and NS strongly suggests that this prolonged hyperpolarization reflects the polysynaptic input from AE onto NS (Rela and Szczupak 2003). Contrary to this general trend, whereas an increase in motor activity was correlated with hyperpolarization of NS, the elongation phase of crawling was correlated with a depolarization. The motoneurons active during elongation also generate inhibitory synaptic responses in NS (Rela and Szczupak 2003), but, during the elongation phase of crawling, NS was depolarized, and the voltage oscillations of NS and CV showed high positive correlation. By virtue of this observation, we propose that NS and CV are subject to a common synaptic input (Fig. 8*B*). Thus, in addition to the electrical coupling, the common input synchronizes their activity and masks the polysynaptic inhibitory effect of CV on NS.

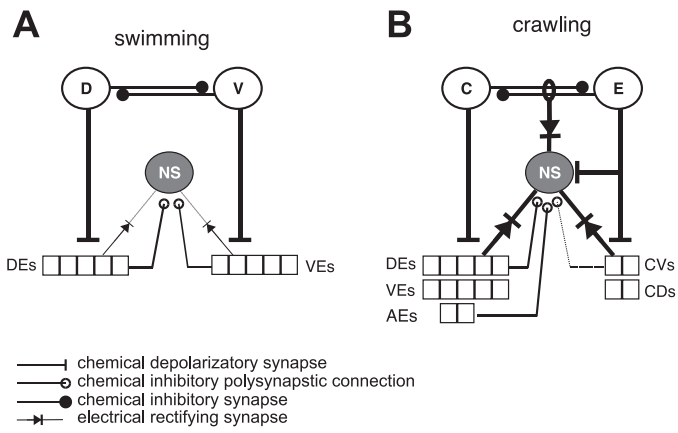

Fig. 8. Schematic network interaction of NS with the swimming and the crawling networks. *A*: the swim CPG, here schematized as D and V for dorsal and ventral phase controls, regulates the activity of the dorsal (DE) and ventral (VE) excitatory motoneurons, respectively. The activity of these motoneurons evokes successive hyperpolarizing signals in NS through chemical inhibitory polysynapstic connections. DEs have a stronger connection than VEs. The rectifying electrical junctions are represented as thin broken lines in virtue of their lack of effect. *B*: the crawling CPG is schematized as C and E for contraction and elongation phase controls. C regulates the simultaneous activity of dorsal and ventral longitudinal excitors and AE motoneurons, and E regulates the simultaneous activity of dorsal and ventral circular (CV and CD) excitors. In addition, the control of the elongation phase is also connected to NS. The longitudinal excitors are connected to NS through polysynaptic inhibitory chemical connections and electrical rectifying junctions. The only effective connection between the circular excitors and NS is through the rectifying electrical junctions. In addition, NS is linked to the CPG, or higher control levels, through electrical rectifying junctions. The thickness of the lines indicates the strength of the connections, and the broken lines indicate that the connection is functionally null.

NS effect on motor patterns. In the course of swimming, Vm_{NS} manipulation had no influence on DE-3 activity. In spite of the fact that in basal conditions hyperpolarization of NS to −80 mV causes a substantial decrease in DE-3 firing (Rodriguez et al. 2009), during swimming it did not affect this parameter. These facts suggest that in the course of this motor pattern the electrical coupling between NS and DE-3, and probably with the rest of the longitudinal excitors, was masked by inputs from the CPG (Fig. 8*A*).

On the contrary, in the course of crawling, manipulation of Vm_{NS} exerted multiple actions on the motor pattern. These effects were observed at the level of the motoneurons and at higher control neurons (e.g., the CPG; Fig. 8*B*).

Hyperpolarization of NS decreased the firing frequency of DE-3 while NS depolarization increased it. The interpretation of these results should take into consideration the rectifying nature of the NS-motoneuron junctions. The fact that hyperpolarizing Vm_{NS} inhibited DE-3 is consistent with the characteristics of the rectifying coupling. However, how should one interpret the effect of NS depolarization? We propose that depolarizing Vm_{NS} counteracts the phasic hyperpolarization that occurs in phase with DE-3 firing (Fig. 3*B*) and therefore its effect on the motoneurons. In terms of the rectifying junctions, depolarization of NS eliminates it from the circuit. According to this interpretation, the depolarization "removes" the inhibitory effect of the phasic NS hyperpolarization and thus magnifies the response to the excitatory input from the CPG (Fig. 8*B*). These results suggest that in the course of crawling, the NS-motoneuron network limits the degree of motoneuron activity.

In addition, we observed that NS hyperpolarization decreased the cycle frequency of crawling, indicating that NS affected the performance of the CPG. Moreover, while depolarization of NS per se did not induce crawling (not shown), depolarization of NS at a fading stage restored it (Fig. 7). These effects could have been achieved by a direct action of NS on

the CPG (Fig. 8*B*) or on gating interneurons upstream from it. Future work should establish the mechanism of action of NS.

Regarding the difference between the effects of NS on swimming and crawling, it is important to take into consideration the different anatomical complexity of the two preparations. Studying the influence of changing Vm_{NS} in a single ganglion for crawling, instead of a chain of multiple ganglia as for swimming, could have led to an underestimation of the role of NS neurons in swimming. On the other hand, while the motor output recorded in the isolated ganglion complies with several features of crawling, it still has to be proven that the network contained in this experimental configuration is the minimal expression of the whole cord crawling network. Future work should address these issues.

NS neurons and their role in motor behaviors. NS neurons have been widely studied in the context of motor control. They have been found to play several functions in insects and arthropods. Among them *1*) NS neurons were described as premotor units that integrate descending signals and transmit these signals to groups of motoneurons (Burrows 1992; Wolf and Buschges 1995); *2*) they were shown to be part of the CPGs of crayfish swimmeret (Mulloney 2003; Paul and Mulloney 1985; Pearson and Fourtner 1974), cockroach walking (Pearson and Fourtner 1974), and crab ventilation (Dicaprio 1989); *3*) NS neurons in the crab have been described as frequency modulators (DiCaprio and Fourtner 1988), regulating the cycle frequency of ventilation; and *4*) in crayfish they were shown to be part of a reflex network that controls the walking motor pattern (Elson et al. 1992; Le Ray and Cattaert 1997).

NS meets the conditions for considering it part of the CPG (Marder and Calabrese 1996): *1*) NS is directly connected to relevant motoneurons; *2*) Vm_{NS} oscillates in phase with the rhythmic activity of the motoneurons; and *3*) changes imposed on Vm_{NS} modify the rhythmic pattern. Because this is the first description of a neuron that can regulate the crawling motor pattern, future work should determine if NS is actually a member of the CPG or a regulatory element.

ACKNOWLEDGMENTS

The authors thank Dr. María Ana Calviño and Lic. Elisa Schneider for helpful discussion of the manuscript.

GRANTS

This work was funded by grants from Agencia Nacional de Investigación Científica y Tecnológica (PICT 2004-1033) and from the University of Buenos Aires (UBACyT X-216) to L. Szczupak.

DISCLOSURES

No conflicts of interest, financial or otherwise, are declared by the author(s).

AUTHOR CONTRIBUTIONS

Author contributions: M.J.R. and R.A. performed experiments; M.J.R., R.A., and L.S. prepared figures; L.S. conception and design of research; L.S. edited and revised manuscript; L.S. approved final version of manuscript.

REFERENCES

Briggman KL, Kristan WB Jr. Imaging dedicated and multifunctional neural circuits generating distinct behaviors. *J Neurosci* 26: 10925–10933, 2006.

Burrows M. Local circuits for the control of leg movements in an insect. *TINS* 15: 226–232, 1992.

Cymbalyuk GS, Gaudry Q, Masino MA, Calabrese RL. Bursting in leech heart interneurons: cell-autonomous and network-based mechanisms. *J Neurosci* 22: 10580–10592, 2002.

Dicaprio RA. Nonspiking interneurons in the ventilatory central pattern generator of the shore crab, Carcinus maenas. *J Comp Neurol* 285: 83–106, 1989.

DiCaprio RA, Fourtner CR. Neural control of ventilation in the shore crab, Carcinus maenas. *J Comp Physiol A* 162: 375–388, 1988.

Eisenhart FJ, Cacciatore TW, Kristan WB. A central pattern generator underlies crawling in the medicinal leech. *J Comp Physiol A* 186: 631–643, 2000.

Elson RC, Sillar KT, Bush BM. Identified proprioceptive afferents and motor rhythm entrainment in the crayfish walking system. *J Neurophysiol* 67: 530–546, 1992.

Fetz EE, Perlmutter SI, Prut Y. Functions of mammalian spinal interneurons during movement. *Current Op Neurobiol* 10: 699–707, 2000.

Gaudry Q, Kristan WB. Behavioral choice by presynaptic inhibition of tactile sensory terminals. *Nat Neurosci* 12: 1450–1457, 2009.

Grillner S. The motor infrastructure: from ion channels to neuronal networks. *Nat Rev Neurosci* 4: 573–586, 2003.

Katz PS. Neurons, networks, and motor behavior. *Neuron* 16: 245–253, 1996.

Kristan WB, Stent GS, Ort CA. Neuronal control of swimming in the medicinal leech: I. Dynamics of the swimming rhythm. *J Comp Physiol* 94: 97–119, 1974.

Le Ray D, Cattaert D. Neural mechanisms of reflex reversal in coxobasipodite depressor motor neurons of the crayfish. *J Neurophysiol* 77: 1963–1978, 1997.

Marder E, Calabrese RL. Principles of rhythmic motor pattern generator. *Phys Rev* 76: 687–717, 1996.

Muller KJ, Nicholls JG, Stent GS. *Neurobiology of the Leech*. Cold Spring Harbor, NY: Cold Spring Harbor Laboratory, 1981.

Mulloney B. During fictive locomotion, graded synaptic currents drive bursts of impulses in swimmeret motor neurons. *J Neurosci* 23: 5953–5962, 2003.

Orlovsky GN, Deliagina TG, Grillner S. *Neuronal Control of Locomotion*. Oxford University Press, 1999.

Ort CA, Kristan WB, Stent GS. Neuronal control of swimming in the medicinal leech. *J Comp Physiol A* 94: 121–154, 1974.

Paul DH, Mulloney B. Nonspiking local interneuron in the motor pattern generator for the crayfish swimmeret. *J Neurophysiol* 54: 28–39, 1985.

Pearson KG, Fourtner CR. Nonspiking interneurons in walking system of the cockroach. *J Neurophysiol* 38: 33–52, 1974.

Perez-Etchegoyen CB, Alvarez RJ, Rodriguez MJ, Szczupak L. The activity of leech motoneurons during motor patterns is regulated by intrinsic properties and synaptic inputs. *J Comp Physiol A* 2011, doi:10.1007/s00359-011-0704-z.

Poppele RBG. Sophisticated spinal contributions to motor control. *TINS* 26: 269–276, 2003.

Puhl JG, Mesce KA. Dopamine activates the motor pattern for crawling in the medicinal leech. *J Neurosci* 28: 4192–4200, 2008.

Rela L, Szczupak L. Coactivation of motoneurons regulated by a network combining electrical and chemical synapses. *J Neurosci* 23: 682–692, 2003.

Rela L, Szczupak L. In situ characterization of a rectifyng electrical junction. *J Neurophysiol* 97: 1405–1412, 2007.

Rodriguez MJ, Perez-Etchegoyen CB, Szczupak L. Premotor nonspiking neurons regulate coupling among motoneurons that innervate overlapping muscle fiber population. *J Comp Physiol A* 195: 1432–1351, 2009.

Stent GS, Kristan WB, Friesen WO, Ort CA, Poon M, Calabrese RL. Neuronal generation of the leech swimming movement. An oscillatory network of neurons driving a locomotory rhythm has been identified. *Science* 200: 1348–1357, 1978.

Stern-Tomlinson W, Nusbaum MP, Perez LE, Kristan WB. A kinematic study of crawling behavior in the leech, hirudo medicinalis. *J Comp Physiol A* 158: 593–603, 1986.

Tresch MC, Saltiel P, dÁvella A, Bizzi E. Coordination and localization in spinal motor systems. *Brain Research Rev* 40: 66–79, 2002.

Wadepuhl M. Depression of excitatory motoneurones by a single neurone in the leech central nervous system. *J Exp Biol* 143: 509–527, 1989.

Wolf H, Buschges A. Nonspiking local interneurons in insect leg motor control. II. Role of nonspiking local interneurons in the control of leg swing during walking. *J Neurophysiol* 73: 1861–1875, 1995.